

# Investigation of the Poly(L-lactide)/Poly(D-lactide) Stereocomplex at the Air–Water Interface by Polarization Modulation Infrared Reflection Absorption Spectroscopy†

Hélène Bourque, Isabelle Laurin, and Michel Pérolet\*

Centre de recherche en sciences et ingénierie des macromolécules, Département de chimie, Université Laval, Cité universitaire, Québec G1K 7P4, Canada

Joy M. Klass,‡ R. Bruce Lennox,‡ and G. Ronald Brown‡,§

Department of Chemistry, McGill University, Montréal, Québec H3A 2K6, and Brock University, St. Catharines, Ontario L2S 3A1, Canada

Received July 11, 2000. In Final Form: July 10, 2001

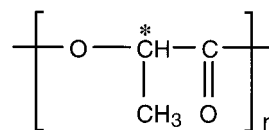
The polarization modulation infrared reflection–absorption spectroscopy (PM-IRRAS) technique has been used in situ to determine the orientation and molecular structure of an equimolar mixture of poly(L-lactide) (PLLA) and poly(D-lactide) (PDLA) spread at the air–water interface. The characteristics of the compression isotherm and of the PM-IRRAS spectra give clear evidence for the presence of a PLLA/PDLA stereocomplex. One of the most striking features in the PM-IRRAS spectra of the stereocomplex is the derivative shape of the band due to the C=O stretching vibration, providing a spectral signature of the presence of polylactide helices oriented parallel to the water surface. The positive and the negative components of the C=O band observed at 1749 and 1765  $\text{cm}^{-1}$  are assigned to the A and E modes of the helical structure, respectively. This assignment was confirmed by recording transmission spectra of the transferred stereocomplex at normal and oblique incidence. Compression of the monolayer past 17  $\text{\AA}^2/\text{repeat unit}$  results in the formation of a bilayer structure. The surface pressure–area isotherm and the PM-IRRAS features suggest that the structure of the film at the air–water interface is similar to the three-dimensional crystal structure of the PLLA/PDLA stereocomplex. In the bulk crystalline structure, the molecules adopt a  $3_1$ -helix conformation, and a segment of a PLLA molecule is paired with a segment of a PDLA molecule, resulting in a racemic unit cell. The PM-IRRAS technique is thus shown to provide detailed insight into the structure of these polymeric Langmuir films and definitely shows that helical polymeric structures can be directly observed at the air–water interface.

## Introduction

Polylactides have been widely studied for use in medical applications because of their bioresorbable and biocompatible properties.<sup>1,2</sup> They can be synthesized either as pure polyenantiomers, poly(L-lactide) (PLLA) or poly(D-lactide) (PDLA) (see Scheme 1), or as copolymers, poly(DL-lactide)s. Various factors such as the chiral unit distribution, crystallinity, and tacticity are known to affect both the biological and physical properties and the kinetics of the degradation of these polymers. Extensive investigations of the chemical and morphological structure of polylactides have been reported.<sup>3–6</sup>

Crystalline PLLA forms left-handed helices<sup>7</sup> while crystalline PDLA adopts right-handed helices.<sup>8</sup> Stereo-

Scheme 1



complex formation from equimolar mixtures of PLLA and PDLA in both melt and solution results in crystal structures and physical properties that differ markedly from those of the individual homopolymers. The PLLA/PDLA stereocomplex exhibits an elevated melting point 50 °C higher than that of the individual homopolymers. Whereas the individual components are optically active, the stereocomplex forms a crystalline structure that is racemic. The stereocomplex crystallizes in a triclinic unit cell, to form a  $3_1$  helical conformation known as the  $\beta$ -form.<sup>8–10</sup> In contrast, the individual polyenantiomers crystallize either in a pseudo-orthorhombic system with two  $10_3$ -helices (known as the  $\alpha$ -form)<sup>7,11–13</sup> or in a “distorted  $3_1$ -helix  $\alpha$ -form”.<sup>10</sup> The  $\beta$ -form of PLLA can also be obtained by changing the conditions used to form fiber samples.<sup>14</sup> The formation, morphology, phase structure,

† This paper is dedicated to the memory of Prof. G. Ronald Brown.

‡ McGill University.

§ Brock University.

\* To whom correspondence should be addressed.

(1) Schindler, A.; Jeffcoat, R.; Kimmel, G. L.; Pitt, C. G.; Wall, M. E.; Zweidinger, R. In *Contemporary Topics in Polymer Science*; Pearce, E. M., Schaeffgen, J. R., Eds.; Plenum Press: New York, 1977; Vol. 2.

(2) Vert, M.; Li, S.; Spenlehauer, G.; Guerin, P. *J. Mater. Sci.: Mater. Med.* **1992**, *3*, 432.

(3) Chabot, F.; Vert, M.; Chapelle, S.; Granger, P. *Polymer* **1983**, *24*, 53.

(4) Schindler, A.; Harper, D. *Polym. Lett.* **1976**, *14*, 729.

(5) Thakur, K. A. M.; Kean, R. T.; Zupfer, J. M.; Buehler, N. U.; Doscoth, M. A.; Munson, E. J. *Macromolecules* **1996**, *29*, 8844.

(6) Cassanas, G.; Kister, G.; Fabregue, E.; Morssli, M.; Bardet, L. *Spectrochim. Acta* **1993**, *49A*, 271.

(7) DeSantis, P.; Kovacs, A. J. *Biopolymers* **1968**, *6*, 209.

(8) Ikada, Y.; Jamshidi, K.; Tsuji, H.; Hyon, S.-H. *Macromolecules* **1987**, *20*, 904.

(9) Okihara, T.; Tsuji, M.; Kawaguchi, A.; Katayama, K.-I.; Tsuji, H.; Hyon, S.-H.; Ikada, Y. *J. Macromol. Sci., Phys.* **1991**, *B30*, 119.

(10) Brizzolara, D.; Cantow, H.-J.; Diederichs, K.; Keller, E.; Domb, A. J. *Macromolecules* **1996**, *29*, 191.

(11) Kister, G.; Cassanas, G.; Vert, M. *Polymer* **1998**, *39*, 267.

(12) Hoogsteen, W.; Postema, A. R.; Pennings, A. J.; ten Brinke, G.; Zugenmaier, P. *Macromolecules* **1990**, *23*, 634.

(13) Qiu, D.; Kean, R. T. *Appl. Spectrosc.* **1998**, *52*, 488.

crystalline structure, and degradability of the stereo-complex and the effect of enantiomeric excess on the formation of the stereocomplex have also been studied.<sup>15,16</sup> The mechanism of stereocomplex formation and the origins of its higher stability are still under active investigation.

The Langmuir film balance technique is particularly useful in distinguishing molecular packing arrangements in two dimensions (2D). For example, Brinkhuis et al.<sup>17</sup> showed that the isotherm for compression of a monolayer of isotactic and syndiotactic poly(methyl methacrylate) (i- and s-PMMA) in a 1:2 ratio exhibits a transition corresponding to the formation of double-helical stereocomplex structures, similar to those formed in the melt and solution. Evidence of the existence of such structures was obtained from effects of the variation of the stoichiometry and tacticity, surface potential behavior, and infrared spectroscopy measurements of films transferred by the Langmuir–Blodgett technique. Investigations of these stereocomplex structures showed that these LB films have a high thermal stability (high melting points) after annealing treatments are applied. Other experiments have shown that the state of aggregation of the i- and s-PMMA molecules in solution strongly affects the monolayer behavior and that it may change with solution storage time.<sup>18</sup>

The polarization modulation infrared reflection–absorption spectroscopy (PM-IRRAS) technique is used here to monitor the compression behavior of equimolar mixtures of PLLA and PDLA deposited at the air–water interface. Of the several techniques used to monitor in situ processes in monolayers at the air–water interface (X-ray and neutron reflectivity, ellipsometry and Brewster angle microscopy, fluorescence microscopy), PM-IRRAS is especially powerful since it provides orientation and conformation information at the molecular level.<sup>19–24</sup> Because the detected signal is differential in nature, PM-IRRAS spectra are almost unaffected by the isotropic absorptions of the sample environment. Moreover, the sign of the bands is directly related to the orientation of the transition moments with respect to the plane of the water subphase.<sup>25,26</sup>

## Materials and Methods

The poly(L-lactide) and poly(D-lactide) samples were synthesized by ring-opening polymerization of L(–)- and D(+)-lactide (Purac Biochem), respectively, using stannous octoate as catalyst and lauryl alcohol as initiator under vacuum at 140 °C for 6 h according to the method of Kleine and Kleine.<sup>27</sup> The resulting

polymers were purified by reprecipitation, using methylene chloride as the solvent and methanol as the precipitant. The mean molecular weights ( $M_w$ ) of the polymers in dioxane, determined by gel permeation chromatography at 35 °C, using a series of Waters styragel HR columns, were found to be  $1.0 \times 10^5$  for poly(L-lactide) and  $1.2 \times 10^5$  for poly(D-lactide). The polydispersities of PLLA and PDLA were 1.8 and 2.9, respectively.

Chloroform (HPLC grade, Sigma-Aldrich) was used as spreading solvent. Subphase water was filtered and deionized in a Nano-Pure Barnstead column (resistivity of 18.3 MΩ·cm).

**Polymer Monolayers.** Monolayer experiments were performed using a KSV 3000 film balance (KSV Instruments, Helsinki, Finland). Surface pressure–area ( $\pi$ – $A$ ) isotherms were recorded using a  $15 \times 58$  cm Teflon trough while transfers of Langmuir–Blodgett (L–B) films were achieved with a  $8 \times 50$  cm Teflon trough with a dipping well. Both troughs were equipped with two hydrophilic, movable barriers that allowed for symmetrical compression. Thermostated water was circulated in the aluminum support of the troughs to control the temperature of the subphase. The experiments were performed at  $35.0 \pm 0.3$  °C. The surface pressure was measured with a precision of  $\pm 0.1$  mN/m using a platinum Wilhelmy plate.

A 1:1 solution mixture of the polyenantomers was prepared by mixing equimolar amounts of each homopolymer in chloroform at a concentration of 0.2 mg/mL. After rigorous cleaning of the water surface, the monolayers were formed by spreading 120  $\mu$ L of the solution (applied to an initial area of 38 Å<sup>2</sup>/repeat unit for the isotherm measurements and 16 Å<sup>2</sup>/repeat unit for the L–B transfers). The organic solvent was allowed to evaporate for 15 min before compression. For all experiments, a compression speed of 1 Å<sup>2</sup>/repeat unit per minute was used. Values of the mean area/repeat unit were calculated using the ratio of the mass applied to the surface and the formula weight of the lactide repeat unit.

Calcium fluoride plates (6 × 25 × 50 mm) were used as substrates for the transfer of L–B films. The plates were first cleaned with chloroform in a bath sonicator for 5 min. Before use, the plates were placed in a plasma cleaner sterilizer (Harrick Scientific Co., Ossining, NY) for 3 min. The substrates were then lowered in the subphase at a depth of 10 mm, and the films were formed as describe above and compressed until a surface pressure of 8 mN/m was reached. After a stabilization period of 30 min, the substrates were raised vertically from the subphase through the compressed films at a speed of 0.1 mm/min. The transfer ratio was always equal to  $1.0 \pm 0.1$ .

**In Situ Infrared Spectroscopy.** The PM-IRRAS spectra at the air–water interface were recorded on an instrument similar to that described by Blaudez et al.<sup>25,26</sup> A schematic representation of the optical and electronic setup is shown in Figure 1. In the optical part of the system, the parallel output beam of the Magna 850 interferometer (Nicolet Instruments, Madison, WI), which was modulated in intensity (between 800 Hz and 1.3 kHz) by the moving mirror, was deflected out of the spectrophotometer by a flat mirror (Passport accessory). The beam was reflected onto a flat mirror toward an off-axis parabolic mirror (3.5 in. focal length) in order to produce a convergent beam. The infrared radiation was p-polarized with a ZnSe wire grid polarizer (Specac) before passing through a photoelastic modulator (Hinds Instruments, type II) operating at a resonance frequency of 37 kHz. The application of a sinusoidal voltage to the modulator crystal induced a modulation between the linear and perpendicular polarization states at a frequency of 74 kHz. This was superimposed to the intensity modulation produced by the interferometer. Following the reflection of the beam at the air–water interface, the radiation was focused, with a ZnSe lens, onto the 1 mm<sup>2</sup> element of a narrow-band MCT detector (Belov Technology, NJ).

The home-built trough (5 × 36 × 0.5 cm) used to spread the monolayers for these experiments was equipped with a Riegler and Kirstein film balance (Germany) using a piece of filter paper (3 × 8 mm, Whatman paper no. 1) as a Wilhelmy plate. It was not possible to accurately measure surface pressures above approximately 30 mN/m with the paper plate. In fact, when the film was compressed above this pressure, the filter paper plate was slowly pushed out of the water subphase and was sometimes completely ejected from the subphase. This may be caused by

(14) Eling, B.; Gogolewski, S.; Pennings, A. J. *Polymer* **1982**, *23*, 1587.

(15) Tsuji, H.; Ikada, Y. *J. Polym. Sci.* **1994**, *53*, 1061 and previous papers in the series.

(16) Brochu, S.; Prud'homme, R. E.; Barakat, I.; Jerome, R. *Macromolecules* **1995**, *28*, 5230.

(17) Brinkhuis, R. H. G.; Schouten, A. J. *Macromolecules* **1992**, *25*, 2725.

(18) Brinkhuis, R. H. G.; Schouten, A. J. *Macromolecules* **1992**, *25*, 2732.

(19) Payan, S.; Desbat, B.; Destrade, C.; Nguyen, H. T. *Langmuir* **1996**, *12*, 6627.

(20) Dicko, A.; Bourque, H.; Pézolet, M. *Chem. Phys. Lipids* **1998**, *96*, 125.

(21) Mao, L.; Ritcey, A. M.; Desbat, B. *Langmuir* **1996**, *12*, 4754.

(22) Huo, Q.; Dziri, L.; Desbat, B.; Russell, K. C.; Leblanc, R. M. *J. Phys. Chem. B* **1999**, *103*, 2929.

(23) Castano, S.; Desbat, B.; Laguerre, M.; Dufourcq, J. *Biochim. Biophys. Acta* **1999**, *1416*, 176.

(24) Ulrich, W.-P.; Vogel, H. *Biophys. J.* **1999**, *76*, 1639.

(25) Blaudez, D.; Turllet, J.-M.; Dufourcq, J.; Bard, D.; Buffeteau, T.; Desbat, B. *J. Chem. Soc., Faraday Trans.* **1996**, *92*, 525.

(26) Blaudez, D.; Buffeteau, T.; Cornut, J. C.; Desbat, B.; Escafre, N.; Pézolet, M.; Turllet, J. M. *Appl. Spectrosc.* **1993**, *47*, 869.

(27) Kleine, J.; Kleine, H. H. *Makromol. Chem.* **1959**, *30*, 23.

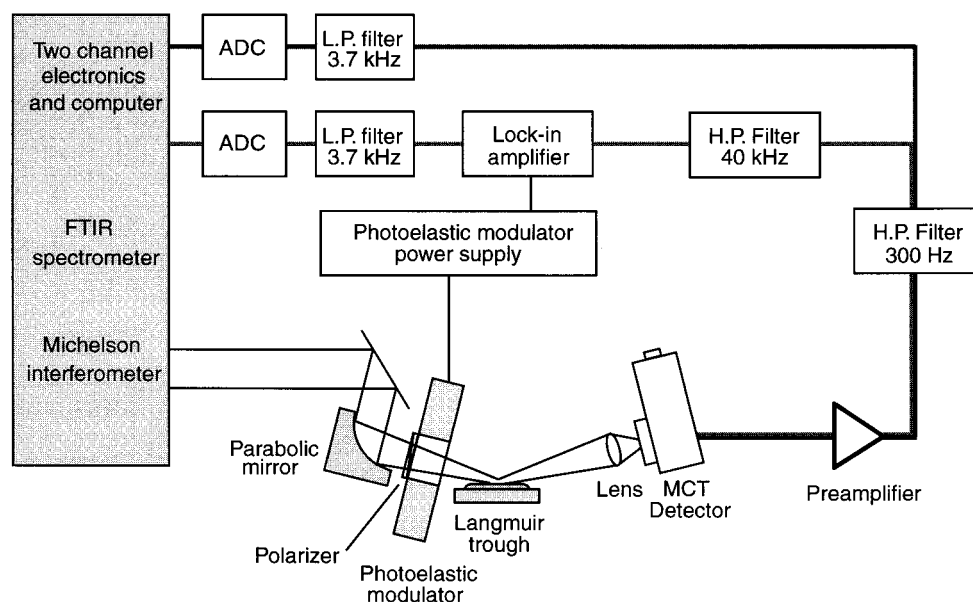


**Figure 1.** Schematic diagram of the optical system and two-channel electronic setup used for PM-IRRAS.

the high stiffness of the film at high surface pressure. The spectrophotometer, the trough, and the optical components sat on an antivibration table. Except for the flat mirror, the trough, and the FTIR spectrophotometer, all components were mounted on inclined aluminum supports to obtain the optimal angle of incidence ( $76^\circ$ ) with respect to the water surface normal.<sup>25,26</sup>

The output of the detector was first amplified with a low-noise preamplifier (Graseby Infrared), mounted near the detector to minimize the noise pick-up, and was then sent to the two-channel electronic instrumentation shown in Figure 1. The detected intensity is the sum of two interferograms, the low-frequency component,  $I_{DC}$

$$I_{DC} = C_{DC}[(R_p + R_s) + J_0(\phi_0)(R_p - R_s)]I_0(\omega_i)$$

which contains the intensity modulation,  $I_0(\omega_i)$ , generated by the interferometer, and the AC component,  $I_{AC}$

$$I_{AC} = C_{AC}[(R_p - R_s)J_2(\phi_0)]I_0(\omega_i) \cos(2\omega_m t)$$

due to the polarization modulation at a frequency of  $2\omega_m$ , induced by the photoelastic modulator. In these equations,  $R_p$  and  $R_s$  are the polarized reflectivities for the infrared radiation polarized parallel and perpendicular to the plane of incidence, respectively,  $J_n$  are  $n$ -order Bessel functions,  $\phi_0$  is the maximum dephasing introduced by the photoelastic modulator crystal at a given wavenumber, and  $C_{DC}$  and  $C_{AC}$  are constants. Since the frequency domain of  $I_{DC}$  is at least 1 order of magnitude lower than that of  $I_{AC}$ , the two components can be separated electronically. The  $I_{DC}$  component was isolated by a dual-channel filter (Stanford Research, model 650) which was set to remove all frequencies below 300 Hz (high-pass filter) and above 10 kHz (low-pass filter). To obtain the demodulated  $I_{AC}$  component, the output signal of the first 300 Hz low-pass filter was sent to a 30 kHz high-pass filter (part of second dual-channel filter), demodulated with a DSP lock-in amplifier (EG&G Instruments model 7260), and finally filtered with a second 10 kHz low-pass filter. The time constant of the lock-in amplifier was adjusted to 80  $\mu$ s. The two signals at the output of the 10 kHz filter were recorded simultaneously using the dual-channel capability of the interferometer and then Fourier transformed to yield the corresponding  $I_{AC}$  and  $I_{DC}$  single-beam spectra. Their ratio gives the PM-IRRAS signal,  $S$ :

$$S = \frac{I_{AC}}{I_{DC}} = C \frac{J_2(\phi_0)(R_p - R_s)}{(R_p + R_s) + J_0(\phi_0)(R_p - R_s)}$$

To obtain the maximum sensitivity, spectra of the covered water surface,  $S(d)$ , were normalized to that of the bare water surface,  $S(0)$ :

$$\frac{\Delta S}{S} = \frac{S(d) - S(0)}{S(0)}$$

The conditions used to prepare the monolayers for the PM-IRRAS measurements were similar to those used for the measurements of the surface pressure–area isotherms on the KSV trough (initial area: 33  $\text{\AA}^2/\text{repeat unit}$ ; temperature: 35  $^\circ\text{C}$ ; compression speed: 1  $\text{\AA}^2/\text{repeat unit per minute}$ ). However, the KSV film balance was operated with continuous compression while the PM-IRRAS film balance was operated in an intermittent compression mode, the surface area being kept constant during the recording of each spectrum. The essential features of the isotherms obtained with the two film balances were the same. All spectra were recorded at a spectral resolution of 4  $\text{cm}^{-1}$ , at a scanning mirror speed of 0.5  $\text{cm/s}$ , and by co-adding 400 interferograms/spectrum. The total acquisition time for each spectrum was about 10 min. Experiments performed with a cutoff optical filter eliminating the infrared radiation above 2000  $\text{cm}^{-1}$  has revealed that no material was squeezed out of the infrared beam due to the heating of the water surface when the filter was not used. All spectra shown below were thus obtained without using a cutoff optical filter.

**ATR and Transmission Infrared Spectroscopy.** The infrared spectrum of the bulk equimolar mixture of the polyanionomers was obtained by attenuated total reflectance (ATR) spectroscopy using a Nicolet Magna 550 spectrophotometer. About 200  $\mu\text{L}$  of the sample solution was spread onto an ATR germanium parallelogram plate ( $50 \times 20 \times 2$  mm, cut at  $45^\circ$  angle) with a Teflon bar. The solvent was allowed to evaporate before measurements were made. The crystal was first cleaned with chloroform and then put in the plasma cleaner sterilizer to remove contaminants. The spectrum was recorded by co-adding 1000 scans at 2  $\text{cm}^{-1}$  resolution using a triangular apodization. Because of its wavelength dependence, the ATR spectrum was reprocessed by using the ATR correction in the Omnic software (Nicolet Instruments, Madison, WI) to correct the band intensities. Polarized transmission spectra of transferred films were recorded using a Nicolet Magna 760 spectrophotometer equipped with a high-sensitivity mercury–cadmium–telluride detector. A total of 1000 scans at a spectral resolution of 4  $\text{cm}^{-1}$  after Happ-Genzel apodization were collected for each spectrum.

## Results and Discussion

**Isotherms.** The  $\pi$ - $A$  isotherm of an equimolar mixture of the polyanionomers spread onto the water subphase



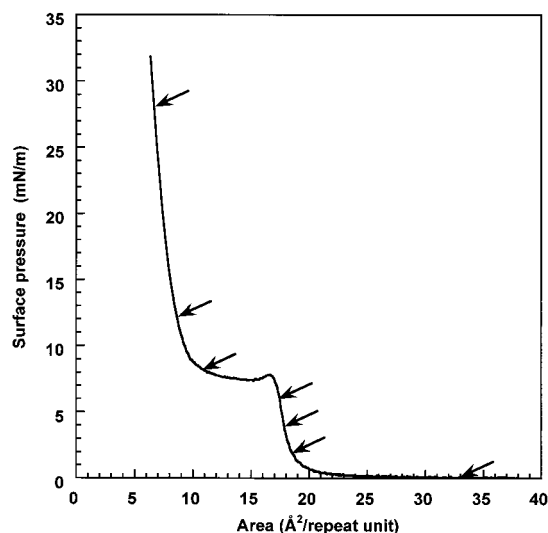


**Figure 2.** Surface pressure–area isotherm of an equimolar mixture of PLLA and PDLA spread at the air–water interface at 35 °C. The arrows indicate the different areas per repeat unit where PM-IRRAS spectra were recorded.

at 35 °C (Figure 2) is distinctly different from those obtained for the individual polyenantionomers.<sup>28</sup> It is reasonable to expect that these differences result from stereocomplex formation. The isotherm of the mixture exhibits at least three distinct regions. At areas  $>25 \text{ Å}^2/\text{repeat unit}$ , no observable changes occur with compression. Finite surface pressure begins at about  $25 \text{ Å}^2/\text{repeat unit}$ , and at approximately  $20 \text{ Å}^2/\text{repeat unit}$  a relatively sharp increase in surface pressure is observed. Extrapolation of the initial rise in surface pressure to 0 mN/m ( $A_{\text{lim1}}$ ) yields an area of  $18.5 \text{ Å}^2/\text{repeat unit}$ . A plateau region ( $\pi = 7.5 \text{ mN/m}$ ) begins at  $17 \text{ Å}^2/\text{repeat unit}$  and continues to about  $11 \text{ Å}^2/\text{repeat unit}$ . This plateau region is followed by a region of sharply increasing surface pressure beginning at  $\sim 10 \text{ Å}^2/\text{repeat unit}$ . The area per repeat unit at this rise is about half that of the first. The inflection point observed prior to the plateau has been interpreted as a kinetic effect related to a change, typically a phase change, for which the conversion rate exceeds the compression rate.<sup>29,30</sup> The surface pressure values just below and above the plateau are less stable than in other regions of the isotherm. The arrows on the isotherm (Figure 2) indicate the different points at which PM-IRRAS spectra were recorded.

Several explanations can be offered to account for the plateau in the isotherm. Such plateaus are often associated with phase transitions and are indicators of phase coexistence. Specific possibilities include the packing of the molecules into a well-defined arrangement, the formation of a bilayer in which the polylactide molecules are forced out of the interface to form a second layer, or a transition during which the polymer adopts a new (e.g., helical) conformation. Of particular note is the possibility that the plateau corresponds to a crystallization process, multilayer formation, or a 2D coil-to-helix transition. Although the  $\pi$ – $A$  curves do not distinguish between these possibilities, the PM-IRRAS spectra presented here do provide insight into the molecular origins of this transition region.

(28) Klass, J. M.; Lennox, R. B.; Brown, G. R.; Bourque, H.; Pérolet, M., to be published.

(29) Brinkhuis, R. H. G.; Schouten, A. J. *Macromolecules* **1991**, *24*, 1487.

(30) Biegajski, J. E.; Cadenhead, D. A.; Prasad, P. N. *Macromolecules* **1991**, *24*, 298.

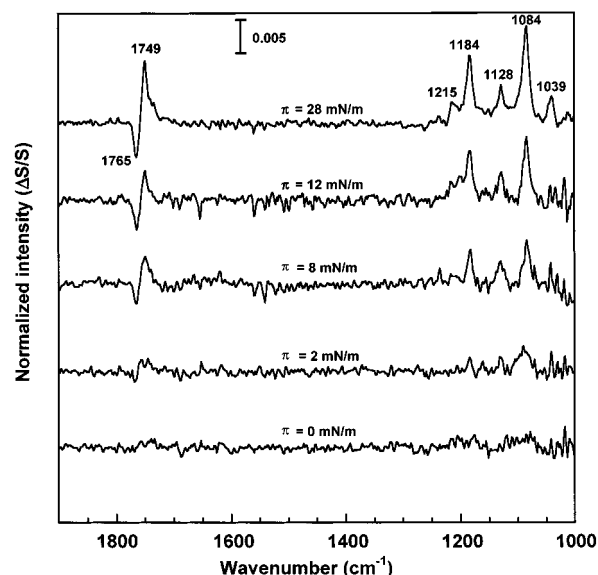


**Figure 3.** Normalized PM-IRRAS spectra of an equimolar mixture of PLLA and PDLA at the air–water interface as a function of surface pressure.

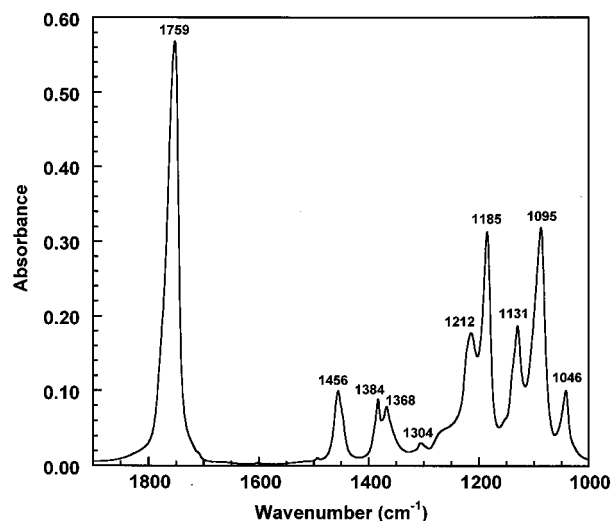


**Figure 4.** ATR spectrum of the bulk PLLA and PDLA stereocomplex at room temperature. The spectrum was corrected for the wavelength dependence of the intensity of the ATR bands.

**PM-IRRAS Spectra.** The normalized PM-IRRAS spectra of the in situ PLLA/PDLA film recorded between 1000 and  $1900 \text{ cm}^{-1}$  at different surface pressures are shown in Figure 3. For comparison, the ATR spectrum of the bulk stereocomplex is shown in Figure 4. The assignment of the observed bands is given in Table 1.

In contrast to the spectrum of the bulk sample (Figure 4), the sign of the bands in the PM-IRRAS spectra can be either positive or negative. A positive band indicates that the transition moment (or a projection thereof) of the associated vibration is in the plane of the water subphase whereas a negative band is indicative of a transition moment (or a projection thereof) which is oriented perpendicular to the water subphase. Spectral simulations<sup>25,26</sup> have established that for a given oscillator the intensity of the band associated with a transition moment parallel to the surface is greater than that associated with the perpendicular orientation.

One of the most striking features in the PM-IRRAS spectra of the stereocomplex is the derivative shape of the

**Table 1. Assignment of the Major Bands in the ATR and PM-IRRAS Spectra of the Stereocomplex**

bulk (cm <sup>-1</sup> )	PM-IRRAS (cm <sup>-1</sup> )	assignment
1046	1039	$\nu(\text{C}-\text{CH}_3)$
1095	1084	$\nu_s(\text{COC})$
1131	1128	$\nu_{as}(\text{CH}_3)$
1185	1184	$\nu_{as}(\text{COC})$
1212	1215	$\nu_{as}(\text{COC})$
1268		$\delta(\text{CH}) + \nu(\text{COC})$
1304		$\delta(\text{CH})$
1368		$\delta(\text{CH}) + \delta_s(\text{CH}_3)$
1384		$\delta_s(\text{CH}_3)$
1456		$\delta_{as}(\text{CH}_3)$
1759	1749 (+)	$\nu(\text{C}=\text{O})$
	1765 (-)	$\nu(\text{C}=\text{O})$

<sup>a</sup> s = symmetric; as = asymmetric; (+) = positive; (-) = negative.

band due to the C=O stretching vibration at finite surface pressure values. It has been shown that such a shape of a PM-IRRAS band can be observed when the transition moment of the vibration associated with the band is oriented at the PM-IRRAS "magic angle" with respect to the normal of the water surface (approximately 40°).<sup>25</sup> For such a case, the PM-IRRAS band is very weak since it results from the superposition of both positive and negative bands. This is clearly not the case for the C=O band around 1755 cm<sup>-1</sup> which has a derivative shape since it is almost the strongest band in the spectrum (Figure 3).

The spectrum of the bulk stereocomplex exhibits a C=O band having an asymmetric band with the maximum intensity at 1759 cm<sup>-1</sup> (Figure 4). The C=O stretching region of the infrared and Raman spectra of polylactides is known to be sensitive to the morphology and the conformation of the polymers.<sup>11</sup> Group theory analysis by Kister et al.<sup>11</sup> shows that the intramolecular vibrational coupling of the C=O groups within the repeat unit of the 3<sub>1</sub> helical structure, expected for the stereocomplex in its crystalline state, should give rise to two components: one with A symmetry (the transition moment along the helix axis) while the other one has E symmetry (the transition moment perpendicular to the helix axis) which is doubly degenerate. These components were clearly observed in the Raman spectra of the bulk stereocomplex as a sharp peak at 1745 cm<sup>-1</sup> (assigned to the A mode) and as broad band around 1760–1780 cm<sup>-1</sup>. This latter band is due to the superposition of the bands associated with the E mode and the amorphous part of the polymer. On the basis of these Raman data, we assign the positive band at 1749 cm<sup>-1</sup> to the A mode and the negative band at 1765 cm<sup>-1</sup> to the doubly degenerate E mode of the helical stereocomplex. As discussed above, for a given oscillator, the intensity of the band associated with a transition moment parallel to the surface is higher than that associated with the perpendicular orientation. Consequently, the PM-IRRAS signal associated with the E mode of the C=O vibration of an isolated helix parallel to the water surface should be slightly positive as opposed to the strong negative band observed. We believe that this is due to the fact that the intermolecular coupling between the polylactide helices in the plane of the film at the air–water interface results in the selective attenuation of the in-plane component of the E mode leaving the out-of-plane component of the E mode unaffected. The transition moment associated with the E mode is then perpendicular to the plane of the film, resulting in a negative PM-IRRAS signal.

To confirm this interpretation of the positive and negative components of the band due to the C=O stretching vibration in the observed PM-IRRAS spectra, polarized transmission spectra of the stereocomplex transferred on

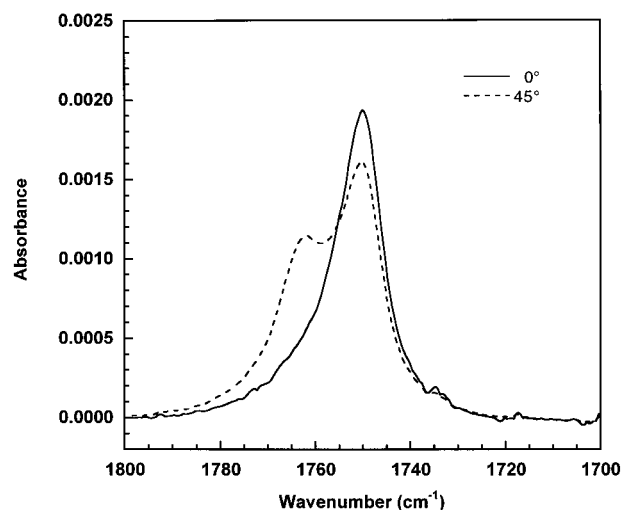


**Figure 5.** Polarized absorbance spectra of a L-B film of the PLLA and PDLA stereocomplex transferred at 8 mN/m at 35 °C. The spectra were recorded at 0° and 45° angle of incidence with the infrared radiation polarized in the plane of incidence (p-polarization).

a calcium fluoride plate at 8 mN/m were recorded at normal and oblique (45°) incidence. The spectra obtained between 1700 and 1800 cm<sup>-1</sup> for the infrared radiation polarized in the plane of incidence (p-polarization) are shown in Figure 5. As can be seen, the 1765 cm<sup>-1</sup> band is very weak in the spectrum recorded at an angle of incidence of 0° but is quite strong in the spectrum recorded at an angle of incidence of 45°. Such a behavior is expected if the transition moment associated with this band is perpendicular to the film, in agreement with the negative PM-IRRAS band observed at 1765 cm<sup>-1</sup>. In addition, the intensity change of the 1749 cm<sup>-1</sup> band with the angle of incidence is as predicted for a vibration with a transition moment in the plane of the film, in agreement with the positive PM-IRRAS band observed at 1749 cm<sup>-1</sup>. These results show unambiguously that the 1749 and 1765 cm<sup>-1</sup> bands are associated with the A and E modes of the polylactide helices in the stereocomplex, respectively, and that these helices lie flat on the water surface. The appearance of such a strong derivative shape PM-IRRAS band has never been reported before, even for  $\alpha$ -helical proteins and polypeptides.<sup>31–33</sup>

These characteristic C=O bands for the stereocomplex are observed even before the onset of surface pressure. Both the area values of this region of the isotherm (20–33 Å<sup>2</sup>/repeat unit) compared to that expected for an isolated lactide residue (20 Å<sup>2</sup>) and the PM-IRRAS spectra suggest that the helices lie parallel to the air–water interface. At surface areas greater than  $A_{\text{lim1}}$  (>18.5 Å<sup>2</sup>/repeat unit), the shape of these two bands is not sufficiently well-defined to offer insight into the film morphology. The sharp band profiles observed after the onset of surface pressure suggest that the population of aligned helices increases with increasing compression.

In the spectral region of the CH<sub>3</sub> and CH bending vibrations (between 1250 and 1400 cm<sup>-1</sup>), the bulk stereocomplex sample exhibits a band near 1456 cm<sup>-1</sup> due to the asymmetric methyl deformation vibration (Figure 4). This band is a specific signature neither of the morphology nor of the conformation of the stereocomplex

(31) Cornut, I.; Desbat, B.; Turlet, J. M.; Dufourcq, J. *Biophys. J.* **1996**, *70*, 305.

(32) Krimm, S.; Bandekar, J. *Adv. Protein Chem.* **1986**, *38*, 181.

(33) Buffeteau, T.; Le Calvez, E.; Castano, S.; Desbat, B.; Blaudez, D.; Dufourcq, J. *J. Phys. Chem. B* **2000**, *104*, 4537.

since it appears in the infrared spectra of all polylactides. The bands with maxima at about 1384, 1368, and 1304  $\text{cm}^{-1}$  are assigned to the  $\delta_s(\text{CH}_3)$  symmetric deformation,  $\delta(\text{CH})$  bending component coupled with the  $\delta_s(\text{CH}_3)$  mode, and  $\delta(\text{CH})$  bending mode, respectively. For the bulk crystalline stereocomplex, deconvolution of these three bands shows that each band is composed of two components assignable to the A and E modes.<sup>11</sup> In the PM-IRRAS spectra shown in Figure 3, no bands are detected in this spectral region. This probably reflects a symmetrical arrangement of the transition moments relative to the helix axis so that all orientations are sampled in the case of the helix lying parallel to air–water interface.

In the spectral region of the skeletal stretching and  $\text{CH}_3$  rocking vibrations (1000–1200  $\text{cm}^{-1}$ ), several absorption bands are present in the PM-IRRAS spectra. The band due to the symmetric C–O–C stretching mode of the ester group appears as a doublet at 1184 and 1215  $\text{cm}^{-1}$ . These correspond to shifts of 1 and 3  $\text{cm}^{-1}$ , respectively, compared to the corresponding bands in the bulk sample spectrum. The band due to the asymmetric C–O–C mode is observed at 1084  $\text{cm}^{-1}$  in the PM-IRRAS spectra but at 1095  $\text{cm}^{-1}$  in the bulk sample spectrum. The 1128 and 1039  $\text{cm}^{-1}$  bands in the PM-IRRAS spectra are assigned to  $\nu_{\text{as}}(\text{CH}_3)$  rocking and  $\nu(\text{C}-\text{CH}_3)$  stretching vibrations, respectively.

The variation of band intensities with the increase in the surface pressure provides additional insight into the structure of the stereocomplex. As the compression proceeds, the intensities of the bands at 1184 and 1084  $\text{cm}^{-1}$  increase concomitantly with those of the C=O bands (1765 and 1749  $\text{cm}^{-1}$ ). Figure 3 shows that the intensity ratios of the 1084 and 1184  $\text{cm}^{-1}$  bands and of the 1749 and 1765  $\text{cm}^{-1}$  bands are almost constant for surface areas larger than 8  $\text{\AA}^2/\text{repeat unit}$  ( $\pi = 12$  mN/m), indicating that the helical structure is maintained to at least 8  $\text{\AA}^2/\text{repeat unit}$ . However, at surface areas less than 8  $\text{\AA}^2/\text{repeat unit}$ , there is an increase in the ratio of the 1749 and 1765  $\text{cm}^{-1}$  band intensities as well as the ratio of the intensities of the 1084 and 1184  $\text{cm}^{-1}$  bands. Furthermore, at 28 mN/m (7  $\text{\AA}^2/\text{repeat unit}$ ), the intensity of the 1749  $\text{cm}^{-1}$  band reaches that of the band associated with the symmetric C–O–C mode at 1184  $\text{cm}^{-1}$ . The intensity of the band due to the  $\nu(\text{C}-\text{CH}_3)$  stretching vibration at 1039  $\text{cm}^{-1}$  also changes with surface pressure. Although the  $\nu(\text{C}-\text{CH}_3)$  band is always present in spectra recorded at high surface pressures, it is not always observed at low surface pressure.

These comments regarding the relative intensities of the PM-IRRAS bands can be further elaborated by combining the PM-IRRAS and isotherm data. The intensity of the PM-IRRAS bands of the film increases with increasing surface concentration. However, the observed intensity depends on both the surface concentration of the absorbing molecules and the orientation of the transition moments responsible for the absorption. Normalization of PM-IRRAS intensities (to unit repeat unit density) ensures that residual changes only reflect changes in orientation of the transitions moments.

The intensity per unit repeat unit density,  $I_N$ , is obtained by dividing the observed intensity,  $I$ , by the number of repeat units per unit area:

$$I_N = \frac{I}{n/A}$$

where  $n$  is the number of repeat units and  $A$  is the trough area. Figure 6 shows the PM-IRRAS intensity per unit

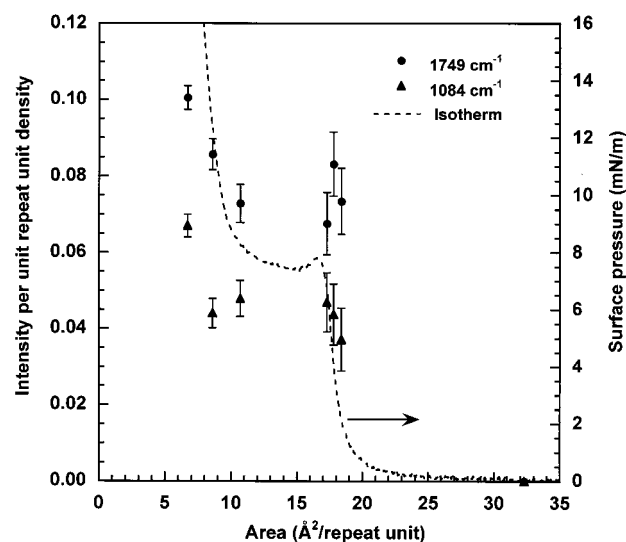


**Figure 6.** Effect of the molecular area per repeat unit on the normalized intensity of the PM-IRRAS bands at 1749  $\text{cm}^{-1}$  (●) and 1084  $\text{cm}^{-1}$  (▲) divided by the number of repeat units per unit area. The isotherm was obtained by continuous compression (see Figure 2) and is shown for reference purposes. The PM-IRRAS data were obtained under conditions of intermittent compression as per the text. The data points represent the mean of at least three measurements, and the error bars are  $\pm 1$  SD about these mean values.

repeat unit density as a function of area per repeat unit for the 1749 and 1084  $\text{cm}^{-1}$  bands. For both bands, the normalized intensity,  $I_N$ , increases markedly as the area is decreased from 35 to 18  $\text{\AA}^2/\text{repeat unit}$ . It then remains essentially constant until a surface area of approximately 10  $\text{\AA}^2/\text{repeat unit}$  is reached. The position of this plateau is in fairly good agreement with that observed on the  $\pi$ - $A$  isotherm (Figure 2). Given that the relative intensity of the PM-IRRAS bands reveals that the helices remain parallel to the surface in the plateau region, the constant  $I_N$  value thus suggests that the film has undergone rearrangement during the plateau region, probably to form a bilayer. Further compression induces a steep rise of  $I_N$ . This indicates that the bilayer is transformed into a more ordered, possibly three-dimensional (3D), crystalline phase. The rigidity of the film at high surface pressures strongly supports the hypothesis of a well-ordered crystalline structure.

The use of  $I_N$  provides structural information that might not otherwise be apparent in the conventional analysis of the intensity of the PM-IRRAS bands. In fact, the increase of the intensity of the PM-IRRAS bands prior to the transition (i.e., at areas  $> 18.5$   $\text{\AA}^2/\text{repeat unit}$ ) is mostly attributable to changes in the orientation of the molecules. At the plateau, however, the PM-IRRAS intensity depends only on the surface concentration of the spread molecules. At high surface densities ( $> 0.13$  repeat units/ $\text{\AA}^2$ ), the increase in  $I_N$  indicates a change in both the film organization and the environment of the polymer helices. Figure 6 also establishes that compression of the film does not cause the helices to adopt orientations that are perpendicular to the air–water interface. Polymer/water and polymer/polymer interactions clearly force the helices to remain aligned and associated with the interface rather than allowing them to adopt other orientations (i.e., perpendicular to the interface) under high pressure. This is noteworthy, since the surface pressure at the monolayer/bilayer transition (i.e., at the plateau) is about 10 atm when converted to an equivalent 3D pressure.



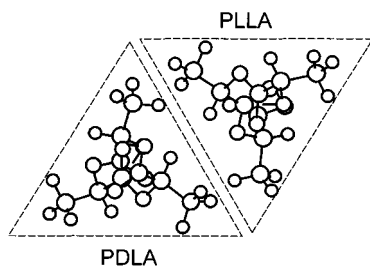


**Figure 7.** End view of the PLLA and PDLA  $3_1$ -helices following the conformation proposed by Okihara et al.<sup>9</sup> and Brizzolara et al.<sup>10</sup> The dotted triangles represent the overall shape of the two  $3_1$ -helices of opposite configuration.

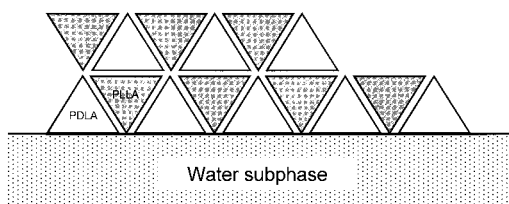


**Figure 8.** Schematic diagram of the crystallization of the PLLA and PDLA stereocomplex bilayer in equilibrium with the monolayer at the air–water interface.

It is interesting to assess the relationship between surface ordering of the stereocomplex helices and the 3D crystallization process. The PLLA/PDLA stereocomplex forms a 3D triclinic crystal with unit cell dimensions:  $a = 0.916$  nm,  $b = 0.916$ ,  $c$  (chain axis) =  $0.870$  nm,  $\alpha = 109.2^\circ$ ,  $\beta = 109.2^\circ$ , and  $\gamma = 109.8^\circ$ .<sup>9,10</sup> The  $3_1$ -helix viewed from a perspective perpendicular to the  $c$ -axis has a cross section that has a triangular appearance due to the arrangement of the methyl groups (see Figure 7).<sup>10</sup> In each unit cell, a segment of a PLLA helix is paired with a segment of a PDLA helix, with methyl groups pointing in the upward direction. The interspaced triangles lead to a parallelepiped array. This organization of the PLLA and PDLA molecules results in a close-packed and well-defined arrangement stabilized by van der Waals interactions. These interactions are probably responsible for the elevated melting point of the stereocomplex ( $50^\circ\text{C}$  higher) compared with the polyenantiomers.

To establish the extent to which the stereocomplexation at the air–water interface is related to the three-dimensional crystallization process, we have estimated the area per repeat unit that a  $3_1$ -helix of PDLA (or PLLA) would occupy. A helix of diameter  $12.5$  Å and pitch of  $8.7$  Å yields an area of  $36.2$  Å<sup>2</sup>/repeat unit. The close-packed arrangement in the model proposed by Brizzolara et al.<sup>10</sup> (Figure 8) leads to the calculated area per repeat unit being reduced to about half of this value, i.e.,  $18$  Å<sup>2</sup>/repeat unit. This is in good agreement with the area value at the inflection point.

This evidence collectively demonstrates that the PLLA and PDLA molecules adopt a helical conformation upon deposition at the air–water interface. Upon compression the helices reorient in the plane of the air–water interface to form a close-packed arrangement. A further decrease in the available surface area leads to a rearrangement of the film (transition region) which produces a second layer (Figure 8). On the basis of the crystal structure of the bulk PLLA/PDLA stereocomplex, this bilayer requires an area of  $9$  Å<sup>2</sup>/repeat unit, in good agreement with the area per repeat unit value at the end of the plateau ( $10$  Å<sup>2</sup>/repeat unit). Further compression results in the formation of a crystalline state, which probably involves a buildup of helices lying parallel to the air–water interface. The

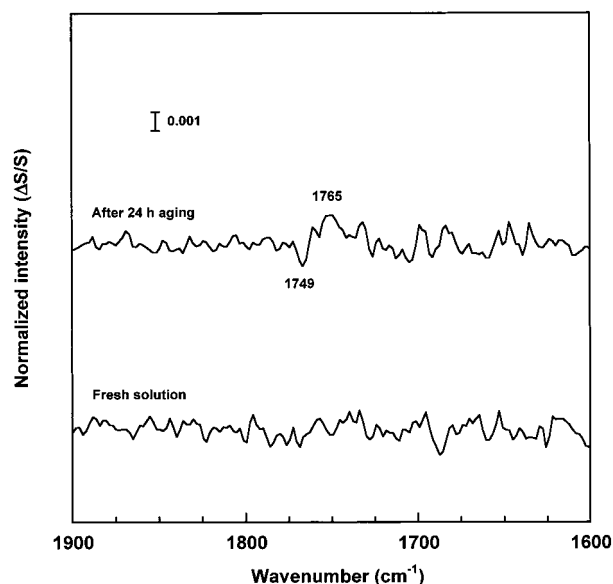


**Figure 9.** Normalized PM-IRRAS spectra of an equimolar mixture of PLLA and PDLA at the air–water interface recorded at  $0$  mN/m as a function of the aging time of the spreading solution.

fact that the band at  $1039$  cm<sup>−1</sup>, associated with the  $\nu$ -(C–CH<sub>3</sub>) stretching vibration, has a greater intensity in the spectra recorded at high surface pressure values suggests that the methyl groups have a specific orientation relative to the water surface (Figure 8). Furthermore, the increase of the intensity ratio of the bands at  $1765$  and  $1749$  cm<sup>−1</sup> and of the bands at  $1184$  and  $1084$  cm<sup>−1</sup> confirms the change in the helix environment and the higher degree of molecular order.

The areas associated with the various isotherm features are consistent with existence of a  $3_1$ -helix as is observed in the 3D stereocomplex. The existence of a stereocomplex at the surface is further supported by the differences observed between the isotherm of the 50:50 mixture and those of the polyenantiomers.<sup>28</sup> A remaining question concerns the timing of stereocomplex formation. Is the stereocomplex formed prior to film spreading (i.e., in the spreading solution), or is it formed (induced) by the film formation process? The spreading solvent used (chloroform) is a complexing solvent.<sup>34</sup> The PM-IRRAS spectra of monolayers formed from an equimolar mixture of PDLA and PLLA and maintained at  $0$  mN/m were studied as a function of storage time of the spreading solution. As seen in Figure 9, the characteristic helix bands (carbonyl bands at  $1749$  and  $1765$  cm<sup>−1</sup>) are observed for the spreading solution stored for 24 h after its preparation but not for the freshly prepared solution. This effect is observed with solutions of the PDLA/PLLA mixture but not for the pure polyenantiomers. The stereocomplex thus appears to have been formed in the spreading solution, rather than during the spreading process. In the case of the compression of a freshly prepared PDLA/PLLA sample spread at the air–water interface, the probability of interaction between the PLLA and PDLA increases as the surface concentration increases. In this case helices first form at the air–water interface and then stereocomplex formation occurs.

## Conclusion

This study demonstrates for the first time that the PLLA/PDLA stereocomplex spontaneously forms helices

(34) Tsuji, H.; Hyon, S.-H.; Ikada, Y. *Macromolecules* **1991**, *24*, 5651.

at the air–water interface. The stereocomplexation process itself can be induced during storage in the casting solution or on deposition at the air–water interface. Compression of the Langmuir film gives a close-packed arrangement of the molecules where the area per repeat unit is reduced by half. Further compression induces the collapse of the film to produce a bilayer. A crystallization process follows bilayer formation as compression continues. Comparison of the experimental area/repeat unit values (obtained from the isotherm) with those estimated from molecular models suggests that the crystallization of the film at the air–water interface is similar to the three-dimensional process. These results clearly demonstrate that PM-IRRAS is a powerful in situ technique to monitor both the secondary structure of polymers at

interfaces and their orientation with respect to the interface.

**Acknowledgment.** The authors are grateful to Prof. Josée Brisson, Department of Chemistry, Laval University, for her help in the drawing of the model of the polylactide stereocomplex and to Prof. Robert E. Prud'homme, Department of Chemistry, Laval University, for helpful discussions. This work was supported by the Natural Sciences and Engineering Research Council of Canada and by the Fonds pour la Formation de Chercheurs et pour l'Aide à la Recherche from the province of Québec (M.P., G.R.B., R.B.L.). J.M.K. thanks Sigma Xi, the Scientific Research Society, for a Grant-in-Aid of Research.

LA0009792